Scale of Texture and its Application to Segmentation

Byung-Woo Hong[1]   Kangyu Ni[2]
Stefano Soatto[1]
Computer Science Department[1], Mathematics Department[2]
University of California Los Angeles, Los Angeles, CA 90095

January 3, 2008

Abstract

This paper examines the issue of scale in modeling texture for the purpose of segmentation. We propose a scale descriptor for texture and an energy minimization model to find the scale of a given texture at each location. For each pixel, we use the intensity distribution in a local patch around that pixel to determine the smallest size of the domain that can be used to generate neighboring patches. The energy functional we propose to minimize is comprised of three terms: The first is the dissimilarity measure using Wasserstein distance or Kullback-Leibler divergence between neighboring patch distributions; the second maximizes the entropy of the local patch, and the third penalizes larger size at equal fidelity. Our experiments show the proposed scale model successfully captures the intrinsic scale of texture at each location. We also apply our scale descriptor for improving texture segmentation based on histogram matching [5].

1   Introduction

A "texture" is a region of the image that exhibits stationary – or cyclostationary – statistics of some sort. If one were to compute the histogram in a region around each pixel, there would be some function of this histogram that is either constant (in practice slowly-varying) or periodic as we move the pixel within the texture. Because the local statistics are pooled from a region around each pixel, a fundamental question in the definition, design, or classification of texture is the area of this region, or "scale". Some statistics are only stationary when computed at a certain scale, but not at larger and/or smaller scales. The "right" scale thus defines the texture, and plays an important role, recognized early in the pioneering work of Julesz [11, 12], with many subsequent attempts to define "elementary texture elements".

Textures are important in the analysis of images, as they provide a mid-level representation that is robust to the actual realization (pixel values) [10, 8, 18, 21], so

1

that "segments" of the image that have a consistent texture can be used as "tokens" [14, 16, 22]; this is also important in image modeling, compression and synthesis [27, 9, 17]. An arsenal of different analytical tools have been brought to bear in the analysis of textures, from statistical models to filtering methods, to geometric approaches. Zhu et al. [27] model texture as a Markov random field (MRF), or equivalently the Gibbs distribution. Efros and Leung [9] observe that textures range in between regular (repeating) and stochastic (without explicit textels) and many synthesis methods often fail in preserving the geometric structures. Their synthesis method is based on a statistical non-parametric model that preserves spatial locality. Inspired by Julesz, Zhu et al. and Wu et al. [25, 23] take a mathematical approach and identify a texture by an equivalence class of statistical features. They later connect this idea with MRF texture models by a minimax entropy scheme [26].

In this work, we address the issue of scale in textures head-on. As [24] point out, the basic texture element, also referred to as "texton" in the MRF literature and considered a fundamental token for pre-attentive visual perception [12], remains a vague concept in need of a better formalization. We provide a characterization of scale that is not restricted to simple statistics, but instead – in a generative framework – we see it as the generator, or "seed," of a texture using any generative model. Rather than texture modeling and classification, therefore, we focus our attention entirely on determining the size a texton in a given image.

In our work, the scale descriptor corresponds to the texton size or texture scale. Many previous works define scale in relation to certain diffusion operators or filters. Lindeberg [13] associates scale with the size of intensity gradient and uses the Gaussian kernel to examine the local scale at each pixel. Brox and Weickert [3] and Strong et al. [20] define scale based on the region size a pixel belongs to. They observe that under the total variation regularization, the intensity change in a pixel is inversely proportional to the region size. In [3], scale is defined as the time taken for a feature to disappear under the TV flow and is applied to accomplish difficult texture segmentation. In [20], scale is the inverse of the intensity change under the TV denoising model [19]. These definitions of scale do not give information on the size of a texton, so we must take a different approach to define scale for textures. For regular (or repeated) textures, scale is the size of the smallest image patch that generates a texture by repeating the patch side by side. Wolf et al. [22] use a patch matching criterion to find texture edges and then incorporate it into a region based active contour model for texture segmentation. Their texture map is successful for segmentation but does not reveal any signs of the correct texton size. For stochastic textures, the spatial relation may not be found and thus may not be obtained by simply stitching textons together. Instead, we take a non-parametric approach and use the entire distribution of the patch to find a texton's size.

For stationary textures, the intrinsic scale is the size of the smallest domain where the distribution is close to that of any other domain of the same size within the texture. Because in practice the statistics may not be strictly stationary, but slowly-varying instead, in practice we look for the smallest local patch whose probability density function (pdf) is similar to the one computed on its neighboring local patches (which we later call "neighboring patch" for short).

Note that the intrinsic scale is not uniform across the image, but it is instead specific

to a given texture. This is in contrast to many schemes for texture segmentation where local pdfs are compared, for instance using the Wasserstein distance [5], but they are computed on a local domain the size of which is fixed throughout the image. If the selected size is smaller than the texton, these schemes over segment the texture; if it is too large, the segmentation may not be accurate because local patches cross over texture boundaries. Not only is the texton size not constant across regions, it may even vary within a texture region, albeit slowly. We believe that by automatically finding the intrinsic scale, histogram-based segmentation will improve its performance. Additionally, the scale can also be added into the data term to distinguish two textons with the same pdf but different scales.

Another potential application of texton scale is inpainting. Texture synthesis by Efros and Leung [9] synthesizes texture one pixel at a time by using the pixel's local patch and looking for similar patches. The size of the patch is defined by the user and is crucial for the performance. The inpainting algorithm in [15] combines both a curvature-based variational inpainting [6] and texture synthesis. The performance also relies on the patch sizes, which are typically selected by the user. By providing the correct scale, this process can be more efficient.

2   Texture Scale

2.1   Notations

Let $I : \Omega \subset R^2 \rightarrow [0, 1]$ be an observed gray-scale image. Define the local patch $\mathcal{R}_{x,r}$ around the pixel point $x = (x_1, x_2) \in \Omega$ with size r ("radius" in analogy to circles) by:

$$\mathcal{R}_{x,r} = \{z \in \Omega \mid \max_{1,2}\{|x_1 - z_1|, |x_2 - z_2|\} < r\} \tag{1}$$

Define the neighboring patch of the local patch by:

$$\mathcal{N}_{x,r} = \mathcal{R}_{x,3r} \backslash \mathcal{R}_{x,r}. \tag{2}$$

The local histogram $h_{\mathcal{R}}(y)$ on $\mathcal{R}$ counts the number of pixels whose intensity is y, for $y \in [0, 1]$:

$$h_{\mathcal{R}}(y) = \int_{\mathcal{R}} \delta(y - I(x))dx, \tag{3}$$

where δ is Dirac's Delta.
Probability density function (or normalized histogram) $P_{\mathcal{R}}$ on $\mathcal{R}$ is the probability of a pixel having value y, for $y \in [0, 1]$:

$$P_{\mathcal{R}}(y) = \frac{\int_{\mathcal{R}} \delta(y - I(x))dx}{\int_{\mathcal{R}} dx}. \tag{4}$$

In this paper, a histogram is assumed to be normalized. The cumulative distribution function $F_{\mathcal{R}}$ describes the probability of a pixel having value less than y, for all $y \in [0, 1]$:

$$F_{\mathcal{R}}(y) = \int_0^y P_{\mathcal{R}}(t)dt. \tag{5}$$

The Wasserstein distance D_W between two probability density functions P_1 and P_2 is:

$$D_W(P_1, P_2) = \int_0^1 |F_1(y) - F_2(y)| dy, \tag{6}$$

where F_1 and F_2 are the corresponding cumulative distribution functions.
The Kullback-Leibler divergence D_{KL} from P_1 to P_2 is:

$$D_{KL}(P_1||P_2) = \int_0^1 P_1(y) \log \frac{P_1(y)}{P_2(y)} dy. \tag{7}$$

The entropy of P is:
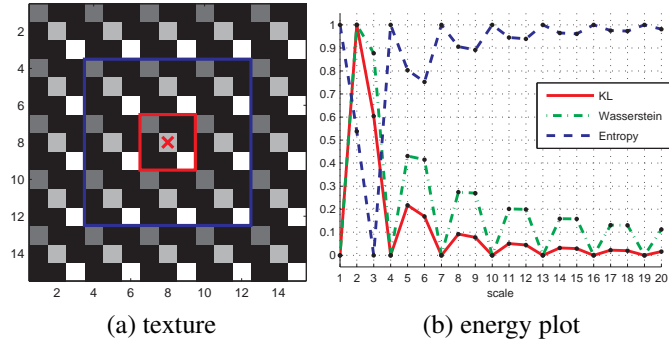
$$H(P) = -\int_0^1 P(y) \log P(y) dy. \tag{8}$$

(a) texture	(b) energy plot

Figure 1: Synthetic texture example: (a) Local patch at 'X' (inside red) and neighboring patch (between red and blue). (b) Energy vs. patch size. Red: histogram difference using the Kullback-Leibler divergence. Green: histogram difference using the Wasserstein distance. Blue: entropy of the local patch histogram

2.2 Description of the scale model

Our proposed scale descriptor is derived by energy minimization of the following model:

$$\inf_r D(P_{\mathcal{R}_{x,r}}, P_{\mathcal{N}_{x,r}}) - \alpha H(P_{\mathcal{R}_{x,r}}) + \beta r(x), \tag{9}$$

where α and β are positive design parameters. In the first term, D is an appropriate measure of the dissimilarity between two probability distributions; for example, we use both the Wasserstein distance D_w and the Kullback-Leibler divergence D_{KL} in

this paper. The first term of this energy function measures the difference between the pdf on the local patch and the pdf on the neighboring patch. Minimizing the difference finds a size whose local patch satisfies the histogram matching criterion. The second term maximizes the entropy of $P_{\mathcal{R}_{x,r}}$, the complexity of the histogram on the local patch. This term avoids selecting homogeneous patches as textons despite their small difference in the pdf with their neighborhood and is necessary because r has to be minimized. The third term penalizes the size r to find the smallest one among all the ones that satisfy the criterion. To understand the proposed model, we show a synthetic texture example and plot the first and second terms versus the patch size r, at the indicated pixels. Fig.1 (a) shows a local patch (in red) around pixel 'X' and a neighboring patch (in between the blue and red curves). In (b), we look at how the first and second terms change with respect to r. The green and red curves are the first terms with Wasserstein distance and Kullback-Leibler divergence, respectively. The blue curve is the entropy of the histogram on the local patch, whose maxima (patch being most complex) appear periodically when r is a multiple of the texton size. Minima (satisfy histogram matching criterion) appear periodically at multiples of r. Therefore, the correct scale should be the smallest among all arguments of the minimum. In this example, the texton size is 1, or a 3×3 patch. The entropy term is redundant in this example but is necessary in general when there are homogeneous areas within the texton.

Fig. 2 is an example consisting of two synthetic textures, on each of which, we select two pixels (A, B and C, D), one closer to the texture edge than the other. From the energy plots, we see that the entropy increases rapidly with patch size as soon as the patch begins to overlap both texture regions. Therefore, measuring the complexity of a local patch's histogram alone is not sufficient to find the scale. The distance between histograms on local patch and neighboring patch also increases rapidly as the local patch begins to overlap both textures, indicating the correct texton size has already been passed. This shows a good sign of using the histogram matching criterion.

The proposed model (9) finds the local scale of a texture. However, it does not attempt to find the scale correctly at locations near texture edges, due to histogram comparison being symmetric. Fig.3 (a) marks three locations, one at the left texture, one near the texture edge, and one on the right texture. The histogram differences by both Wasserstein distance in (c) and Kullback-Leibler divergence in (d) attain local minima periodically because both local and neighboring patches are almost symmetric about the texture edge when the patch size is large. Therefore, histogram comparison must be modified in order to find the correct scale especially for the pixels in the vicinity of the boundary of different textures. We propose the following modification of model (9):

$$\inf_{r} D^*(P_{\mathcal{R}_{x,r}}, P_{\mathcal{N}_{x,r}}) - \alpha H(P_{\mathcal{R}_{x,r}}) + \beta r(x) \qquad (10)$$

$$D^*(P_{\mathcal{R}_{x,r}}, P_{\mathcal{N}_{x,r}}) = \min_{i} D(P_{\mathcal{R}_{x,r}}, P_{\mathcal{N}_{x,r,i}}), \qquad (11)$$

where $\mathcal{N}_{x,r,i}$ is a sub-neighboring patch within $\mathcal{N}_{x,r}$ whose size is r. For computational efficiency, 8 sub-neighboring patches are pre-defined as follows:
$\{\mathcal{R}_{(x_1+2r,x_2+2r),r}, \mathcal{R}_{(x_1,x_2+2r),r}, \mathcal{R}_{(x_1-2r,x_2+2r),r}, \mathcal{R}_{(x_1-2r,x_2),r},$
$\mathcal{R}_{(x_1-2r,x_2-2r),r}, \mathcal{R}_{(x_1,x_2-2r),r}, \mathcal{R}_{(x_1+2r,x_2-2r),r}, \mathcal{R}_{(x_1+2r,x_2),r}\}.$

Numerically, the proposed models are solved in the discrete setting. It is difficult to derive the Euler-Lagrange equation of the energy functional in (9) and (10) because histograms depend on the variable r. As also seen in the energy plots, the proposed model has many local minima, thus the steepest descent method does not find a global minimum.

3   Texture Segmentation

In this section, we utilize scale and propose an unsupervised texture segmentation mode. Our model is adapted from the histogram based segmentation [5], a two-phase nonparametric region-based active contour that uses local histograms as image features. The model partitions the image domain into two regions so that the local histograms within each region are similar to one another. In [5], the local histograms have a uniform patch size and we propose to use an adaptive scale. Moreover, we use scale as an image feature in the segmentation model. We give an example to show scale plays an important role. Fig.4 (a) is an image consisting of two textures with the same histogram but different scales. The segmentation result in (a) is by two-phase piecewise constant active contour model [7], indicated by the intensities black and white. The partition is within textons and do not distinguish textures, because two textures have the same intensity mean. In (b), we show the partition using histogram based segmentation model with global scale $r = 1$. The partition captures the inner texture but also falsely includes partial outer texture, because the scale is too small for the outer region. In (c), the global scale $r = 4$ is large enough and two textures are considered the same because they have the same histogram. To distinguish them, scale has to be added as an image feature in the segmentation model. The proposed model uses scale for characterizing histograms (as an image feature) and also as an image feature:

$$
\min_{0 \le u \le 1, P_1, P_2, r_1, r_2} \int_\Omega |\nabla u| \tag{12}
$$
$$
+ \int_\Omega [\lambda_1 D_w(P_1, P_{x,r(x)}) + \lambda_2 (r_1 - r(x))^2] u(x) dx
$$
$$
+ \lambda \int_\Omega [\lambda_1 D_w(P_2, P_{x,r(x)}) + \lambda_2 (r_2 - r(x))^2](1 - u(x)) dx,
$$

where λ_1 and λ_2 are positive parameters. Minimizing this energy functional separates the image domain into two so that the local histograms within each region are similar to one another and the scale intensities are similar within each region. The first term penalizes the total length of the object boundary. The second and third are fidelity terms. They minimize the integral over all pixels inside their respective regions of distance between a constant (optimal) histogram and the local histograms and distance between a constant (optimal) value and the scale intensities. The partition is obtained by the following thresholding: $\Omega = \{u \le 0.5\} \cup \{u > 0.5\}$.
The minimization can be approximated by a three-step scheme, using the methods in [1] and [2]. First, fix $u, r_1,$ and r_2 and minimize with respect to F_1 and F_2 and calculus of variation gives:

$$\int u(x) \frac{F_1(y) - F_{x,r(x)}(y)}{|F_1(y) - F_{x,r(x)}(y)|} dx = 0$$

and

$$\int [1 - u(x)] \frac{F_2(y) - F_{x,r(x)}(y)}{|F_2(y) - F_{x,r(x)}(y)|} dx = 0,$$

respectively, for each $0 \le y \le L$. Therefore,

$$\begin{aligned} F_1(y) = \text{ weighted median of } F_{x,r(x)}(y) \\ \text{with weight } u(x), \end{aligned} \tag{13}$$

and

$$\begin{aligned} F_2(y) = \text{ weighted median of } F_{x,r(x)}(y) \\ \text{with weight } (1 - u(x)). \end{aligned} \tag{14}$$

Second, fix u, F_1, and F_2 and minimize with respect to r_1 and r_2 gives

$$r_1 = \int_\Omega r(x) u(x) dx / \int_\Omega u(x) dx, \tag{15}$$

and

$$r_2 = \int_\Omega r(x)(1 - u(x)) dx / \int_\Omega u(x) dx. \tag{16}$$

Third, fix F_1 and F_2 and minimize with respect to u. By using the methods in [1] and [2], we may avoid a stiff minimization that involves the mean curvature flow of u. Decouple (12) by adding a new variable v in a convex term:

$$\begin{aligned} \min_{u, 0 \le v \le 1} & \int_\Omega |\nabla u(x)| dx + \frac{1}{2\theta} \int_\Omega (u(x) - v(x))^2 dx \\ & + \int_\Omega f(x) v(x) dx \ , \end{aligned} \tag{17}$$

where $f(x) = \lambda_1 \int_0^L |F_1(y) - F_{x,r(x)}(y)| - |F_2(y) - F_{x,r(x)}(y)| dy + \lambda_2 [(r_1 - r(x))^2 - (r_2 - r(x))^2]$.
Minimize the convex variational model (17) by solving the coupled problems, alternately:

$$\min_u \int_\Omega |\nabla u(x)| + \frac{1}{2\theta}(u(x) - v(x))^2 dx \tag{18}$$

7

$$\min_{0 \le v \le 1} \frac{1}{2\theta} \int_{\Omega} (u(x) - v(x))^2 dx$$
$$+\lambda \int_{\Omega} f(x)v(x)dx \tag{19}$$

Equation (18) can be solved efficiently by the Chambolle's method [4], based on the dual formulation of the total variation norm:

$$u(x) = v(x) - \theta \mathrm{div}p(x) \ , \tag{20}$$

where $p = (p^1, p^2)$ solves $\nabla(\theta \mathrm{div}p - v) - |\nabla(\theta \mathrm{div}p - v)|p = 0$ and is solved by a fixed point method,

$$p^{n+1} = \frac{p^n + \delta t \nabla(\mathrm{div}p^n - v/\theta)}{1 + \delta t |(\mathrm{div}p^n - v/\theta)|}. \tag{21}$$

The solution of (19) is [2]:

$$v(x) = \max\{\min\{u(x) - \theta\lambda f(x), 1\}, 0\} \ . \tag{22}$$

The minimization scheme is to iterate (13), (14), (15), (16), (21), (20), and (22) alternately, until convergence.

4   Experiments

We first show experimental results of the proposed scale model on several Brodatz textures. Fig.5(a) shows three arbitrarily chosen pixels on a Brodatz texture. In (b), the curve of entropy versus patch size at each indicated pixel is almost increasing and does not have a global maximum as patch size continues to increase. The histograms gain complexity as the patch size increases and there is no clear sign of the correct scale according to these curves, which emphasizes that entropy alone is not enough to find the scale. On the contrary, in (d), we see the histogram difference (using the Wasserstein distance) versus patch size obtains a global minimum and the texton size can be clearly identified at the first minimum from left, away from $r = 0$. In (c), the scale at each indicated pixel by the proposed model with the Wasserstein distance is accurate. In (f), the histogram difference versus patch size plot shows the Kullback-Leibler divergence captures the characteristics to some extend but not as well as the Wasserstein distance. The selected scale shown in (e) is roughly correct. The reason of the Wasserstein distance outperforming the Kullback-Leibler divergence in this experiment is that the Wasserstein distance overcomes the deficiency of pointwise metrics, as addressed in [5].

Fig.6 shows five Brodatz textures in column (a) and their scale maps by Tikhonov flow [13] in column (b), by TV flow [3] in column (c), and by the proposed model

in column (d). The scale maps for these textures are expected to be homogeneous and only our model captures this characteristic. The parameters are $\alpha = 0.001$ and $\beta = 0.1$ in (9) for all five textures. We show in column (a) the scales obtained by our model at three arbitrarily selected locations are accurate and agree with human perception. In the first row, the scale map by Tikhonov flow highlights the edge of circles because the scale is associated with intensity gradients. The scale map by TV flow (d) highlights the circle regions since the scale is proportional to the size of a homogeneous region. Neither of the previous scale descriptors describe the size of the texture. We also apply the proposed scale model to several natural images from the Berkeley Segmentation Dataset as shown in the following.

Fig.7, 8, and 9 compare the histogram based segmentation model with global scales [5] and the proposed model. Column (a) shows the given natural images. Columns (b), (c), and (d) are the segmentation results by [5] with global scale $r = 4, 16$, and 32, respectively. In (b) with $r = 4$, the segmentation selects within the cheetah patterns at some locations because the global scale is too small for those locations. In (c) (with $r = 16$) and in (d) (with $r = 32$), segmentation does not partition within the cheetah patterns but does not fall on the boundary accurately. This is because the global scale is too large, resulting many patches cross over both regions. The scale maps in (e) describe correctly each object region by a homogeneous scale and each background region by another homogeneous scale. The results in (f) by the proposed model that utilizes scale improve the segmentation result significantly.
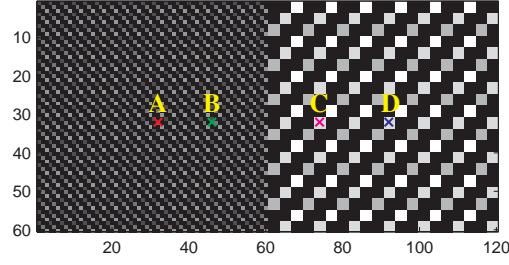
5 Discussion and Conclusion

In this work, we define a scale descriptor associated with texture. We propose a non-parametric model that seeks the scale by matching histograms in a self-repeating manner. The proposed energy functional consists of three terms. The first finds a size that satisfies a histogram matching criterion that compares the local patch with the neighboring patch. The second maximizes the complexity of a patch to avoid choosing the wrong size when there are homogeneous regions within a texton. The third penalizes the size because texton is the smallest element that generates a texture. We show that these three terms are not redundant to one another. We also propose a modified model suited for finding the scale near the texture edges. Our experimental results show that the scale map of a texture by the proposed model is highly accurate. Furthermore, we use scale as an image feature and also use it for characterizing local histograms. Our experimental results on several natural images show an improvement in texture segmentation over approaches that rely on a fixed scale.
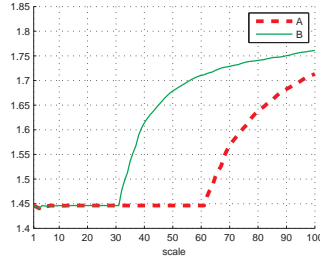
References

[1] J. F. Aujol, G. Gilboa, T. F. Chan, and O. S. Structure-texture image decomposition - modeling, algorithms, and parameter selection. *IJCV*, 67(1):151–167, 2006. 6, 7

[2] X. Bresson, T. F. Chan, P. Vandergheynst, J. P. Thiran, and S. Osher. Fast global minimization of the active contour/snake model. *J. of Math. Imaging and Vision*, 28(2):151–167, 2007. 6, 7, 8

[3] T. Brox and J. Weickert. A tv flow based local scale measure for texture discrimination. *Proc. of ECCV*, 2004. 2, 8

[4] A. Chambolle. An algorithm for total variation minimization and applications. *J. of Math. Imaging and Vision*, 20:89–97, 2004. 8

[5] T. Chan, S. Esedoglu, and K. Ni. Histogram based segmentation using wasserstein distances. In *Proc. of Scale Space and Variational Methods in Computer Vision*, volume 4485/2007, pages 697–708, 2007. 1, 3, 6, 8, 9

[6] T. F. Chan, S. H. Kang, and J. Shen. Euler's elastica and curvature based inpainting. *SIAM journal on Applied Mathematics*, 63(2):564–592, 2002. 3

[7] T. F. Chan and L. A. Vese. Active contours without edges. *IEEE Trans. on Image Processing*, 10(2):266–277, 2001. 6, 13

[8] C. C. Chen and R. C. Dubes. Discrete mrf model parameters as features for texture classification. *IEEE Int'l Conf. on Systems, Man and Cybernetics*, 4(7):1–6, 1990. 1

[9] A. Efros and T. Leung. Texture synthesis by non-parametric sampling. *ICCV*, 2:1033–1038, 1999. 2, 3

[10] I. Fogel and D. Sagi. Gabor filters as texture discriminator. *Journ. of Biological Cybernetics*, 61(2):103–113, 1989. 1

[11] B. Julesz. Visual pattern discrimination. *IEEE Trans. on Information Theory*, 8:84–92, 1962. 1

[12] B. Julesz. Textons, the elements of texture perception and their interatcions. *Nature*, 290:91–97, 1981. 1, 2

[13] T. Lindeberg. Principles for automatic scale selection. In *Handbook on Computer Vision and Applications*, volume 2, pages 239–274. 1999. 2, 8

[14] J. Malik and P. Perona. A computational model of texture segmentation. *Proc. of CVPR*, pages 326–332, 1989. 2

[15] K. Ni, D. Roble, and T. F. Chan. A texture synthesis approach to elastica inpainting. *SIGGRAPH Sketches*, 2007. 3

[16] N. Paragios and R. Deriche. Geodesic active regions and level set methods for supervised texture segmentation. *Int'l Journ. of Computer Vision*, 46(3):223–247, 2002. 2

[17] J. Portilla and E. P. Simoncelli. A parametric texture model based on joint statistics of complex wavelet coefficients. *Int'l Journ. of Computer Vision*, 40(1):1018–1024, 2000. 2

[18] Y. Rubner and C. Tomasi. Texture-based image retrieval without segmentation. *ICCV*, 2:1018–1024, 1999. 1

[19] L. I. Rudin, S. Osher, and E. Fatemi. Nonlinear total variation based noise removal algorithms. *Physica*, D(60):259–268, 1992. 2

[20] D. Strong, J. Aujol, and T. Chan. Scale recognition, regularization parameter selection, and meyer's g norm in total variation regularization. *UCLA CAM Report 05-02*, 2005. 2

[21] M. Verma and A. Zisserman. A statistical approach to texture classification from single images. *IJCV*, 62(1-2), 2005. 1

[22] L. Wolf, X. Huang, I. Martin, and M. Dimitris. Patch-based texture edges and segmentation. *Proc. of ECCV 2006*, 3952/2006:481–493, 2006. 2

[23] Y. N. Wu, S. C. Zhu, and X. W. Liu. Equivalence of julesz ensemble and frame models. *IJCV*, 38(3), 2000. 2

[24] S. C. Zhu, C. Guo, Y. Wang, and Z. Xu. What are textons? *IJCV*, 27(2):121–143, 2005. 2

[25] S. C. Zhu, X. W. Liu, and Y. N. Wu. Exploring julesz ensembles by efficient markov chain monte carlo–towards a trichromacy theory of texture. *PAMI*, 22(6), 2000. 2

[26] S. C. Zhu, Y. Wu, and D. B. Mumford. Minimax etropy principles and its applications to texture modeling. *Neural Computation*, 9:1627–1660, 1997. 2
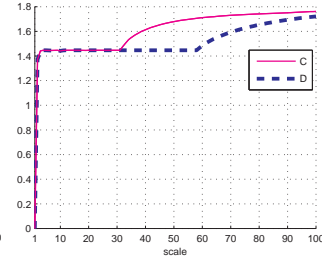
[27] S. C. Zhu, Y. N. Wu, and D. Mumford. Filters, random fields and maximum entropy (frame). *Int'l Journ. of Compt. Vision*, 27(2):1–20, 1998. 2
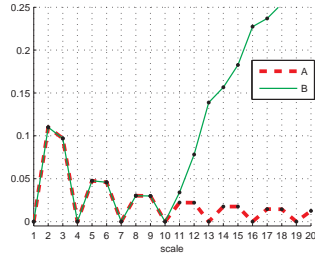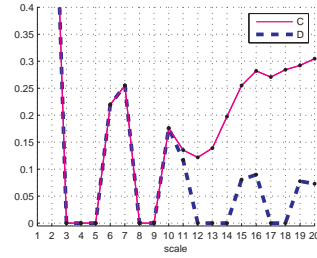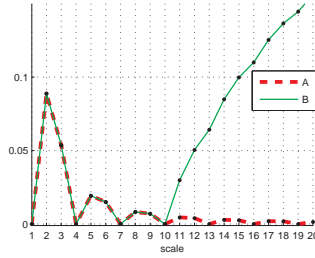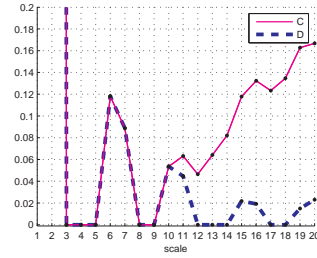
(a) Two textures

(b) Entropy

(c) Entropy

(d) Wasserstein

(e) Wasserstein

(f) KL divergence

(g) KL divergence

Figure 2: Image consisting of two synthetic textures. (a) Mark two locations A, B on the left texture and two locations C, D on the right. (b) Entropy vs. size of local patch at A and B. (c) Entropy vs. size of local patch at C and D. (d) Histogram difference vs. size with Kullback-Leibler divergence at A and B. (e) Histogram difference vs. size with Kullback-Leibler divergence at C and D. (f) Histogram difference vs. size with Wasserstein distance at A and B. (g) Histogram difference vs. size with Wasserstein distance at C and D

12

(a) Location B at texture edge   (b) Entropy

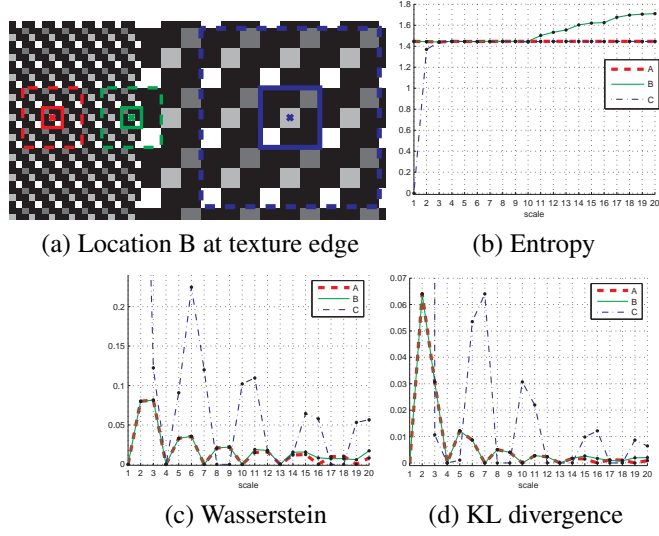(c) Wasserstein   (d) KL divergence

Figure 3: Image consisting of two synthetic textures. (a) Mark three locations A on the left texture, B near the texture edge and B on the right. (b) Entropy vs. size of local patch at each location. (c) Histogram difference vs. size with Kullback-Leibler divergence at each location. (d) Histogram difference vs. size with Kullback-Leibler divergence at each location.

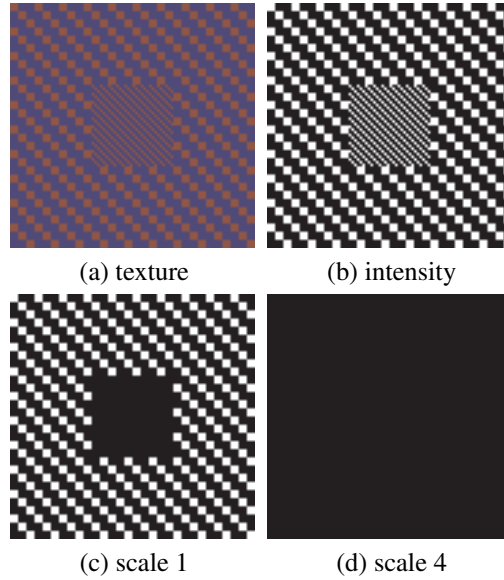(a) texture   (b) intensity

(c) scale 1   (d) scale 4

Figure 4: (a) Image consisting of two synthetic textures with the same histogram but different scales. (b) Segmentation by using intensity [7]. (c) Histogram based segmentation with scale $r = 1$. (d) Histogram based segmentation with scale $r = 4$.

(a) Brodatz texture   (b) Entropy

(c) Local scales   (d) Wasserstein

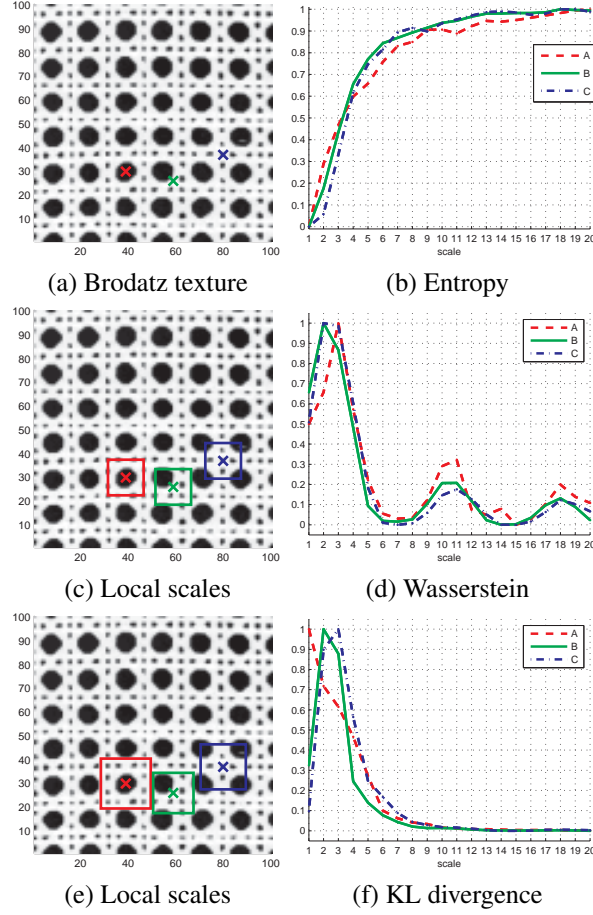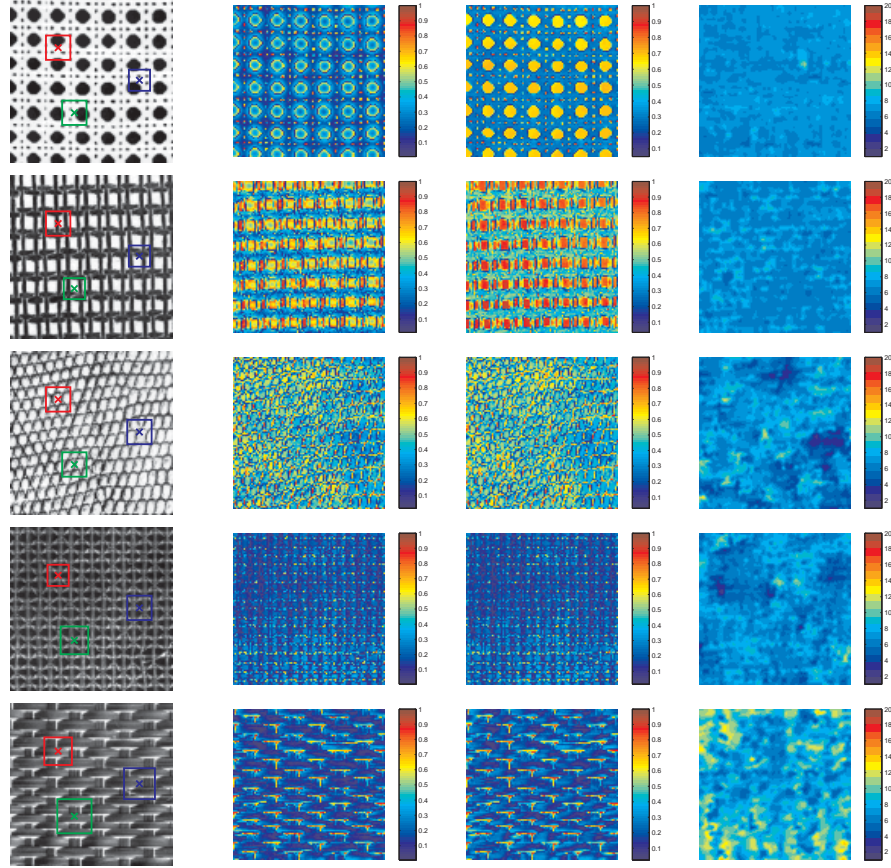(e) Local scales   (f) KL divergence

Figure 5: Brodatz texture image. (a) Mark three locations A, B, and C. (b) Entropy vs. size of local patch at A, B, and C. (c) Selected scales by proposed model using Wasserstein distance at A, B, and C. (d) Histogram difference vs. size with Wasserstein distance at A, B, and C. (e) Selected scales by proposed model using Kullback-Leibler divergence at A, B, and C. (f) Histogram difference vs. size with Wasserstein distance at A, B, and C. (g) Histogram difference vs. size with Kullback-Leibler divergence at A, B, and C.

14

(a) Brodatz textures (b) Tikhonov scale map (c) TV scale map (d) Proposed scale map

Figure 6: Comparison of scale maps with other methods on Brodatz texture images.
(a) Brodatz texture images with patches with texton scales obtained by our model at
arbitrarily selected pixels. (b) Scale map by Tikhonov flow. (c) Scale map by TV flow.
(d) Scale map by the proposed model with $\alpha = 0.001$ and $\beta = 0.1$.

15

(a) Image   (b) Scale map   (c) Proposed model
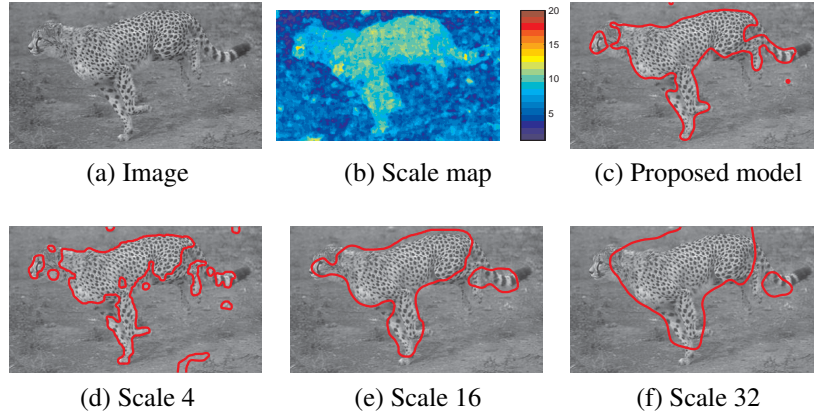
(d) Scale 4   (e) Scale 16   (f) Scale 32

Figure 7: (a) Original Image. (b) Scale map by the proposed model. (c) Segmentation by proposed model. (d) Segmentation with global scale $r = 4$. (e) Segmentation with global scale $r = 16$. (f) Segmentation with global scale $r = 32$.

(a) Image   (b) Scale map   (c) Proposed model

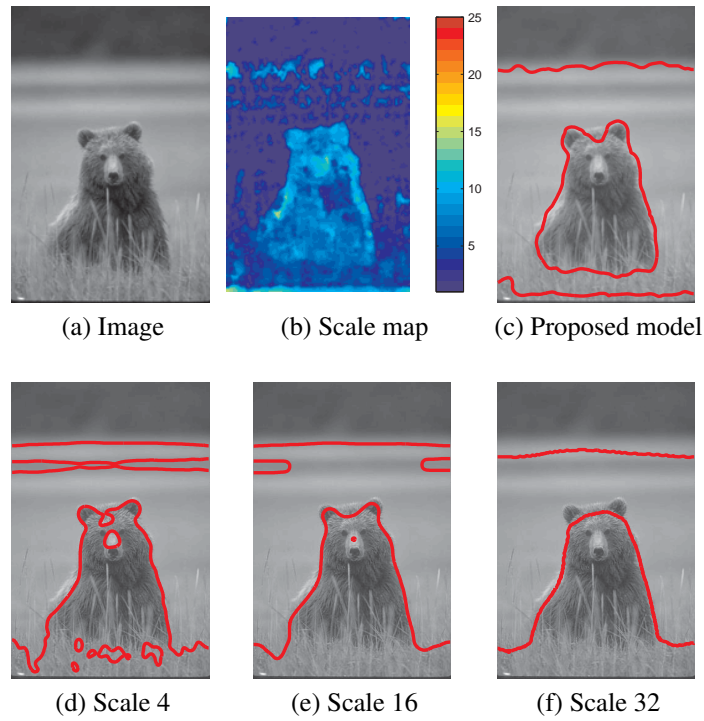(d) Scale 4   (e) Scale 16   (f) Scale 32

Figure 8: (a) Original Image. (b) Scale map by the proposed model. (c) Segmentation by proposed model. (d) Segmentation with global scale $r = 4$. (e) Segmentation with global scale $r = 16$. (f) Segmentation with global scale $r = 32$.

(a) Image   (b) Scale map   (c) Proposed model
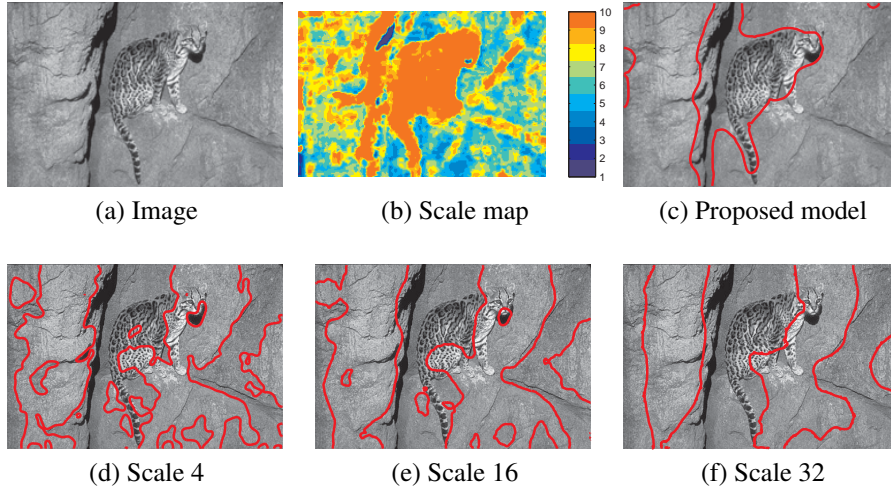
(d) Scale 4   (e) Scale 16   (f) Scale 32

Figure 9: (a) Original Image. (b) Scale map by the proposed model. (c) Segmentation by proposed model. (d) Segmentation with global scale $r = 4$. (e) Segmentation with global scale $r = 16$. (f) Segmentation with global scale $r = 32$.